JLab Program Advisory Committee Eleven Proposal Cover Sheet

This document must be received by close of business on Wednesday, December 18, 1996 at:

Jefferson Lab
User Liaison Office, Mail Stop 12 B
12000 Jefferson Avenue
Newport News, VA 23606

(Choose one)

☐ **New Proposal Title:** Extension to E93021: The Charged Pion Form Factor

☐ **Update Experiment Number:**

☐ **Letter-of-Intent Title:**

Contact Person

Name: David Mack
Institution: TJNAF
Address: MS 12H
Address: 12000 Jefferson Avenue
City, State ZIP/Country: Newport News, VA 23606
Phone: (757) 269-7442 **FAX:** (757) 269-7363
E-Mail › Internet: MACK@JLAB.ORG

Experimental Hall: C **Days Requested for Approval:** 12.7

Jefferson Lab Use Only

Receipt Date: 15 DEC 96

By: L. Arnold PR 96-007

HAZARD IDENTIFICATION CHECKLIST

CEBAF Experiment: _____ Date: 12/18/96

Check all items for which there is an anticipated need—do not check items that are part of the CEBAF standard experiment (HRSE, HRSH, CLAS, HMS, SOS in standard configurations).

Cryogenics _____ beamline magnets _____ analysis magnets _____ target _____ drift chambers _____ other	**Electrical Equipment** _____ cryo/electrical devices _____ capacitor banks _____ high voltage _____ exposed equipment	**Radioactive/Hazardous Materials** List any radioactive or hazadorous/ toxic materials planned for use: _____ _____
Pressure Vessels _____ inside diameter _____ operating pressure _____ window material _____ window thickness	**Flammable Gas or Liquids** (incl. target) type: _____ flow rate: _____ capacity: _____	**Other Target Materials** ___ Beryllium (Be) ___ Lithium (Li) ___ Mercury (Hg) ___ Lead (Pb) ___ Tungsten (W) ___ Uranium (U) ___ Other (list below) _____ _____
Vacuum Vessels _____ inside diameter _____ operating pressure _____ window material _____ window thickness	**Radioactive Sources** _____ permanent installation _____ temporary use type: _____ strength: _____	**Large Mech. Structure/System** _____ lifting devices _____ motion controllers _____ scaffolding or elevated platforms _____ other
Lasers type: _____ wattage: _____ class: _____ **Installation** _____ permanent _____ temporary **Use** _____ calibration _____ alignment	**Hazardous Materials** ___ cyanide plating materials ___ scintillation oil (from) ___ PCBs ___ methane ___ TMAE ___ TEA ___ photographic developers ___ other (list below) _____ _____ _____	**Notes:** standard HMS standard SOS standard cryotarget standard beamline _____ _____

LAB RESOURCES REQUIREMENTS LIST

CEBAF Proposal No.: _____ Date: 12/18/96
(For CEBAF User Liaison Office use only.)

List below significant resources — both equipment and human — that you are requesting *from CEBAF* in support of mounting and executing the proposed experiment. Do not include items that will be routinely supplied to all running experiments, such as the base equipment for the hall and technical support for routine operation, installation, and maintenance.

Major Installations *(either your equip. or new equip. requested from CEBAF)*

HMS Quad string must be pulled back to reach 10.5°. These magnets must be resurveyed. The downstream beam pipe supports need modification to avoid hitting the HMS. The new HMS slit-box must also be surveyed.

New Support Structures: _____

Data Acquisition/Reduction

Computing Resources: _____

New Software: _____

Major Equipment

Magnets _____

Power Supplies _____

Targets _____

Detectors _____

Electronics _____

Computer Hardware _____

Other _____

Other

BEAM REQUIREMENTS LIST

JLab Proposal No.: _____ Date: 12/18/96

Hall: C Anticipated Run Date: Fall 1997 PAC Approved Days: _____

Spokesperson: Mack, Huber, Blok Hall Liaison: Mack
Phone: x7442
E-mail: mack@JLAB.ORG

List all combinations of anticipated targets and beam conditions required to execute the experiment. (This list will form the primary basis for the Radiation Safety Assesment Document (RSAD) calculations that must be performed for each experiment.)

Condition No.	Beam Energy (MeV)	Mean Beam Current (μA)	Polarization and Other Special Requirements (e.g., time structure)	Target Material (use multiple rows for complex targets — e.g., w/windows)	Material Thickness (mg/cm²)	Est. Beam-On Time for Cond. No. (hours)
$Q^2 = 2.4$	3545	100	none	Time shared between 4cm LH_2 and 4cm LD_2	LH_2: 312	90
	4545	"			LD_2: 624	50
$Q^2 = 3.2$	4045	"				110
	5045	"				60

The beam energies, E_{Beam}, available are: $E_{Beam} = N \times E_{Linac}$ where N = 1, 2, 3, 4, or 5. E_{Linac} = 800 MeV, i.e., available E_{Beam} are 800, 1600, 2400, 3200, and 4000 MeV. Other energies should be arranged with the Hall Leader before listing.

Extension to E93-021: The Charged Pion Form Factor

D. Abbott, R. Carlini, J. Dunne, R. Ent, D. Mack (Cospokesperson),
D. Meekins, J. Mitchell, A. Saha, W. Vulcan, S. Wood, C. Yan
Physics Division, TJNAF

O.K. Baker*, K. Assamagan, C. Keppel*, L.G. Tang*
Physics Department, Hampton University
Hampton, Virginia
(and Physics Division, TJNAF)*

K. Gustafsson
University of Maryland
College Park, MD

C.W. de Jager, G. van der Steenhoven
NIKHEF-K
Amsterdam, The Netherlands

H. Blok (Cospokesperson), J. Volmer
Faculteit Natuur- en Sterrenkunde, Vrije Universiteit
Amsterdam, The Netherlands

G.E. Dodge, A. Klein, L.M. Qin, P. Ulmer, K. Vansyoc
Old Dominion University
Norfolk, Virginia

D. Koltenuk
Physics Department, University of Pennsylvania
Philadelphia, Pennsylvania

G. Adams, V. Frolov, J. Napolitano, J. Price, P. Stoler
Physics Department, Renssalaer Polytechnic Institute
Troy, New York

E.J. Brash, G.M. Huber (Cospokesperson), G.J. Lolos, Z. Papandreou, M. Serdarevic, D. Zainea
Department of Physics, University of Regina
Regina, SK, Canada

C. Armstrong, J. Finn
College of William and Mary
Williamsburg, VA

H. Mkrtchyan, A. Gasparyan, Ts. Amatuni
Yerevan Physics Institute
Yerevan, Armenia

Abstract

As part of a program to determine the charged pion form factor at Q^2 = .5 - 5 $(GeV/c)^2$, we now request approval for measurements which require beam energies between 4 and 5 GeV. Assuming the dominance of t-channel one pion exchange in the charged pion forward longitudinal response, the charged pion form factor F_π can be determined. The measurements of F_π proposed here would dramatically improve on the existing data set and provide an important test of soft predictions in the transition between soft and perturbative regimes. Model tests are proposed as well to search for physics backgrounds which may be present in the longitudinal response. Measurements in Hall C at Q^2 of .5, .75, 1.0, and 1.6 are already approved (E93-021) and scheduled for Fall 1997. We request time to extend those measurements to Q^2 = 2.4 and 3.2 during the same running cycle because 5 GeV beam should be available.

1 Introduction

This extension request contains only a fraction of the background material from the original E93-021 proposal. Please refer to that document if needed. This document is mainly concerned with updating the experimental issues since we now possess two years of operational experience in Hall C, and have even completed a short $(e, e'\pi)$ test run.

One of the great hopes for research at TJNAF is that it will lead to a better understanding of QCD between the non-perturbative and perturbative regimes. Improvement in our knowledge of F_π, the pion charge form factor, would be an important step. Although the pion is not an easy experimental target, it is a simpler object than the nucleon. Perturbative QCD descriptions of elastic form factors should be valid at much lower Q^2 for the pion than for the nucleon since the former contains one fewer quark. In fact, for $Q^2 \simeq 4$ $(GeV/c)^2$, roughly half the F_π amplitude may be due to pQCD contributions. Another feature which makes the pion case particularly interesting is that the pion β-decay constant f_π normalizes the asymptotic form factor $Q^2 F_\pi$. No such independent normalization exists for G_M^P, which is a function of the (unknown) proton structure function. Existing data on G_M^P at up to Q^2=30 $(GeV/c)^2$ are also believed by some authors to be very far from asymptotia.

New data for F_π covering the Q^2 range .5 - 5. $(GeV/c)^2$ with combined statistical, systematic, and model errors of order 10% would dramatically improve the F_π data base, and would allow one to distinguish between existing treatments of soft contributions.

1.1 Previous Experiments

1.1.1 Data

Although this field has been dormant since the late 1970's, the field was quite mature at that time. Hence, we briefly review here some of the hard lessons learned by our predecessors.

The first major work largely above the baryon resonance region (W > 2 GeV) was by Brown *et al.* at the Cambridge Electron Accelerator ("CEA") [3]. The longitudinal response could not be extracted model independently since only high ϵ data were taken. The model of Berends [4] which

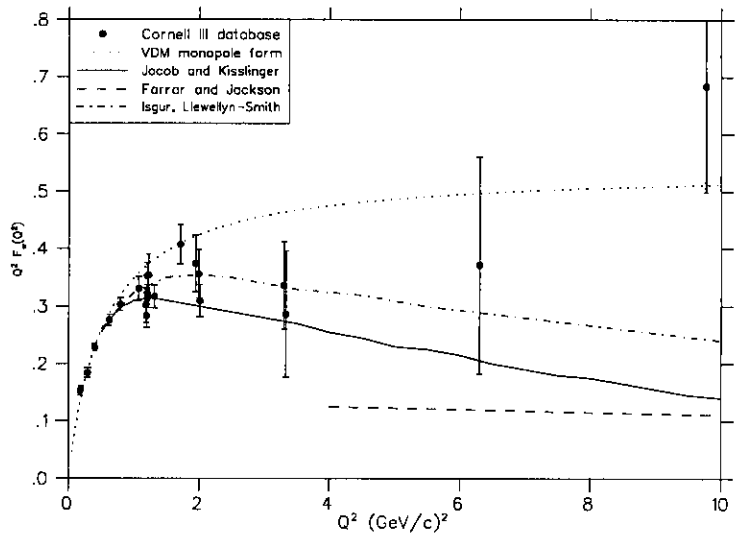

Figure 1: F_π from electroproduction measurements (Cornell III).

assumes purely isovector photons was fitted to the unseparated $\sigma_T + \epsilon\sigma_L$ data with F_π as the only free parameter. Between this and a similar experiment at Cornell by Bebek *et al.* [5] ("Cornell I"), values of F_π were obtained for Q^2 = .18 - 2.01 $(GeV/c)^2$.

Later work at Cornell ("Cornell II") on a deuterium target demonstrated that a significant isoscalar component existed in the unseparated response, $\sigma_T + \epsilon\sigma_L$ [6]. Because it was believed this isoscalar component should be subtracted before comparison to the model, the old CEA and Cornell I values of F_π were reanalyzed and lowered by 3%-7% with the smaller (larger) corrections at the smaller (larger) end of the Q^2 range. Hence the Cornell II analysis superseded the older CEA and Cornell I analyses.

The next Cornell experiment ("Cornell III") acquired only low ϵ data, but by using earlier high ϵ measurements where available (CEA, Cornell I, and Cornell II) they separated σ_T and σ_L for the first time. It was discovered that the model of Berends grossly underpredicted σ_T at $Q^2 > 1$ $(GeV/c)^2$. Although the poor description of σ_T did not have a large effect on F_π at low Q^2 where $\sigma_L \gg \sigma_T$, the model error meant that the Cornell II F_π values were still too high. The Cornell III values for F_π, valued for their large Q^2 coverage, are found in Figure 1.

No subtraction of isoscalar backgrounds was made in the Cornell III analysis; it was assumed that the isoscalar backgrounds identified in the unseparated Cornell II data were primarily of transverse nature. While Cornell III data provide the best available estimates of F_π at the larger Q^2 values, large extrapolations in W and Q^2 (between different experiments!) were required. Indeed, it is fair to say that no real measurements of σ_L exist at Q^2 above 3.33 $(GeV/c)^2$.

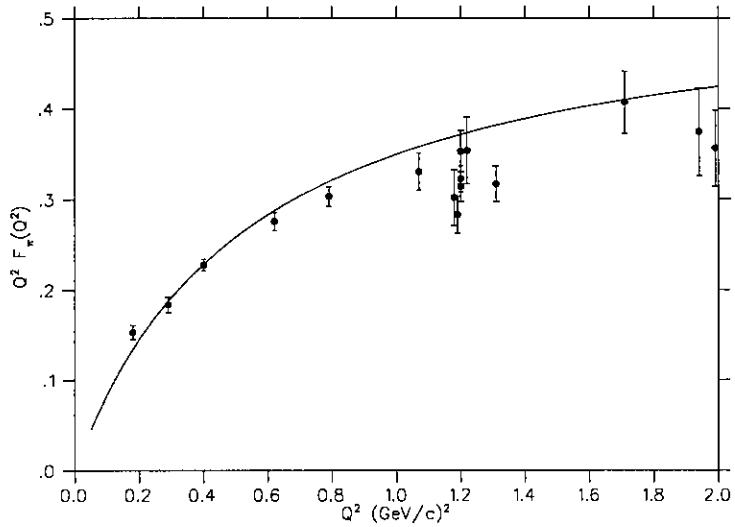

Figure 2: F_π at low Q^2. The solid line is a monopole form factor fitted by Amendolia *et al.* to elastic pion-electron scattering.

1.1.2 Model Tests

It is of some interest to compare F_π derived from electroproduction and elastic scattering measurements. The lowest electroproduction point at $Q^2 = .18$ lies about 2.3 standard deviations above a monopole fit through the elastic data. (Figure 2) Above the Q^2 range of the elastic measurements, however, there are points at Q^2= .29, .4, .62, and .79 all which agree extremely well with the monopole fit. This gives us some confidence that the extraction of F_π from electroproduction data is not pathologically model dependent, at least in this Q^2 region.

One might wonder whether a measurement on a bound nucleon in deuterium gives the same result as on a free nucleon. Bebek *et al.* [6] have shown that, to within their statistical errors, the yield of π^+ at Q^2=1.2 and small $-t$ is the same for both targets. No corrections were made in the analysis other than to use a wider missing mass cut for the deuterium target to account for Fermi motion.

One piece of evidence that backgrounds in σ_L are small, and that t-pole dominance applies at not-so-small values of $-t$, is seen in Figure 3 [6]. Using *unseparated* data, the experimenters determined F_π at two Q^2 values, using data covering a wide range of $-t_{min}$ values. For example, at Q^2=2, consistent values of F_π were obtained using kinematic settings such that $-t_{min}$ ranged from -3.5m_π^2 to -8m_π^2. This latter value is quite far from the pole, and gives us confidence that we may be able to do even better using data with *separated* σ_L.

We turn now to the ratios $\sigma(\pi^-)/\sigma(\pi^+)$. If there are no isoscalar backgrounds, then we expect R_L= 1. Existing electroproduction data [2] show the *unseparated* ratio R at $-t$ = .1 to be slightly less than 1, decreasing at larger values of $-t$. (The errors are of order $\pm$10%) While these data

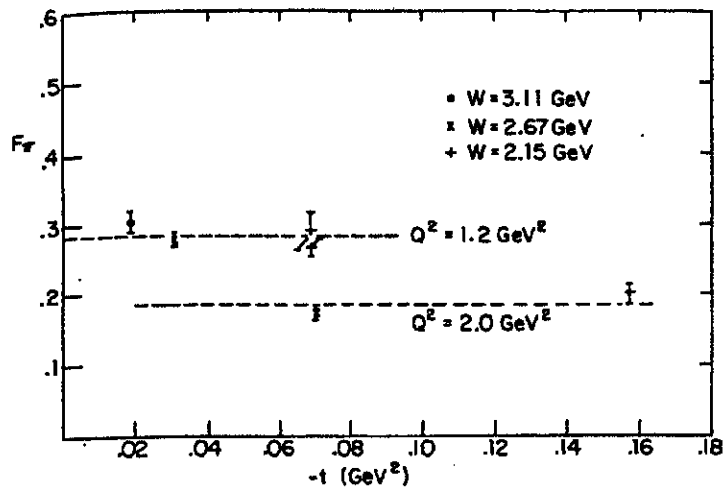

Figure 3: Dependence of the extracted F_π on $-t_{min}$. From Cornell II.

are consistent with a two-component model in which $R_L = 1$ at small $-t$ where σ_L dominates, and $R_T \simeq .25$ at large $-t$ where σ_L has died away, they are nevertheless inconclusive. Separated ratios R_L would be much more sensitive to the presence of isoscalar backgrounds.

With increasing Q^2, backgrounds due to interactions with valence quarks must become more important. Nachtmann [8] has predicted that s-channel quark diagrams will cause R_T to approach 1/4. This is because π^- production is due to interaction with d quarks (q=1/3) and π^+ with u quarks (q=2/3), so $R_T \propto ((1/3)/(2/3))^2 = 1/4$. The *separated* ratio R_T has been obtained with very large error bars [2], and the data weakly support $R_T = 1/4$. More accurate measurements of R_T (and R_L) would help us to understand the reaction mechanism for pion electroproduction at high Q^2.

1.2 Theory

1.2.1 F_π Predictions

Isgur and Llewellyn Smith [9] have argued that so-called hard (pQCD) contributions to the nucleon magnetic form factor G_M^N are only of order 1% for $Q^2 = 4\ (GeV/c)^2$. Similar arguments by the same authors suggest that hard contributions to F_π at the same Q^2 may be of order 50%. The reason for this is that while at least two gluons must be exchanged to hold the nucleon together during elastic scattering, a single gluon need only be exchanged in the case of the pion. Each gluon

exchange makes the Q^2 needed to achieve the pQCD limit higher by the factor $(\alpha_s/\pi)^{-n}$, where n is the number of exchanged gluons, and α_s is the QCD coupling constant. This suggests that the pion may be the better laboratory for pQCD inspired studies of elastic form factors. Data at higher Q^2 than can be achieved at TJNAF, say Q^2= 15, could test even the most conservative estimates of asymptotic F_π.

Accurate F_π data in the TJNAF Q^2 region of this proposal would provide important tests of QCD in the non-perturbative regime. Estimates of soft contributions by Isgur *et al.* [9] exhibit simple, testable features which lie within reach of TJNAF Q^2 range. The calculations predict a steep rise between 0 and 1.5 $(GeV/c)^2$, where a peak is reached. Above this peak the predictions decrease slowly. (See Figure 1, dot-dash curve.) Radyushkin and collaborators have performed QCD sum rule calculations of the pion wave function and electric form factor F_π. [10, 11] Their calculations relate F_π to parameters of the pion wave function called nonlocal condensates. TJNAF measurements would be directly comparable to such sum rule calculations also.

Jacob and Kisslinger [12] have attempted to describe F_π using a Bethe-Salpeter equation. Their model consists of a linear confining potential which dominates at low Q^2 and a perturbative part which dominates at high Q^2. The asymptotic prediction is that of Farrar and Jackson [13], (long dashed line, Figure 1), and is a rigorous QCD result. The three free parameters of the model (the quark mass, the strength parameter, and the strong coupling constant) are fixed by the normalization $F_\pi(0)$=1.0, the pion decay constant f_π, and the pion rms radius $< r_\pi^2 >^{1/2}$. Thus the model must trivially agree with the F_π data at low Q^2, will describe F_π at asymptotic Q^2 if QCD is valid, and may describe the data at intermediate Q^2 if the model and approximations are any good. The interesting prediction is made (see figure 1, solid line) that Q^2F_π will peak near Q^2=1 and decrease fairly rapidly with Q^2, becoming essentially asymptotic by Q^2=15. Above Q^2=1 the poor quality data suggest, if anything, that the calculation decreases too rapidly. Better quality data are clearly needed for $Q^2 \geq 1$. A Bethe-Salpeter equation model has also been investigated by Ito *et al.* [14]

Lattice gauge calculations have had some modest success in describing F_π at $Q^2 \leq 1$ [16]. Nevertheless, statistical and systematic errors in the calculations are large compared to the data in the range. There are presently no plans to extend these calculations to higher Q^2 [17], although this would be very interesting.

To summarize, much can be learned at TJNAF about the usefulness of QCD sum rule and relativistic potential model applications to the pion in the (presumably) difficult and non-perturbative Q^2 regime of 1 - 5 $(GeV/c)^2$.

2 The Experiment

This examination of previous experiments, as well as the physics background considerations discussed in the Theory section, suggest several obvious ways in which a quality measurement of F_π could be done at TJNAF:

- Take high statistics data. This was not possible with the earlier low duty factor machines, and will make systematic errors easier to identify and control.

- At low Q^2 values, make careful measurements of $d\sigma_L/dt$ in $p(e,e'\pi^+)n$ for $-t \simeq +m_\pi^2$ in order to constrain the $g_{\pi NN}$ form factor. This will be attempted in the already approved time for E93-021.

- Perform a separation of σ_L and σ_T for $p(e,e'\pi^+)n$ and $d(e,e'\pi^\pm)NN_s$. This decouples the F_π determination from the much more complicated transverse cross section. Do this in a manner which minimizes error amplification and extrapolation in Q^2 and W (eg, take the low and high ϵ points with the same apparatus during the same experiment).

- Measure the ratio $\sigma_L(\gamma_v + p \rightarrow \pi^+ + n)/\ \sigma_L(\gamma_v + n \rightarrow \pi^- + p)$ using a deuterium target to test for isoscalar backgrounds near the pion pole. This may also be useful for identifying pQCD backgrounds.

- Measure forward π^0 production (ie, backward proton production) in $\gamma_v + p \rightarrow p + \pi^0$ to look for pQCD background contributions to σ_L.

- Finally, where isoscalar or pQCD physics backgrounds are shown to be small, see whether σ_L is well described by the Born term model. If so, proceed to extract F_π.

In this experiment we will make coincidence measurements between charged pions or protons in the HMS and electrons in the SOS. Since the HMS will detect pions along the direction of $\vec{q}$, the dominant contribution will be due to the pion pole diagram. Only events with θ_{pq} near zero degrees are useful, so a high luminosity spectrometer system like the HMS-SOS is well suited to the measurement. Because σ_L must be separated, two beam energies are needed for each Q^2.

Table 1 contains the actual performance of each spectrometer for momenta typical of this experiment. Both spectrometers will be operated with pt-pt tunes in Y (ie, large solid angle mode). These are the standard tunes for both spectrometers and the matrix elements and acceptances are well understood. Because the HMS will be operated in small angle mode (θ_{min} = 10.5 degrees) with the quad string pulled back 40 cm, its tune must be modified slightly. The change in the optics is straightforward (a reduction in the strength of the quads) [20] and new matrix elements will take little time to generate. Target angle resolution will deteriorate by a geometric factor given roughly by the relative increase in distance of Q1 to the target. A new collimator will be built and surveyed into place which maintains the existing HMS x'tgt and y'tgt acceptances.

Small HMS angles are essential for reasonable coverage in ϵ because of the relatively low SOS maximum momentum of 1.8 GeV/c. The small angle HMS mode is required for the already approved and scheduled low Q^2 measurements, and does not represent new overhead for the high Q^2 measurements.

Table 1: Performance of the HMS (pt-to-pt, small angle mode) and SOS (pt-to-pt). Resolutions are all σ. The solid angle is defined by octagonal apertures of densimet in both arms.

	$\Delta p/p$	$dx'tgt$ (mrad)	$dy'tgt$ (mrad)	$dYtgt$ (cm)	Δp (GeV/c)	$\Delta\Theta$ (mrad)	$\Delta\Phi$ (mrad)	$\Delta\Omega$ (msr)
HMS	$.6{\cdot}10^{-3}$	1.5	.7	.15	±10%	±69.5	±27.2	6.62
SOS	$.7{\cdot}10^{-3}$	.2	2.	.20	± 15%	±37.5	±57.5	7.55

A liquid hydrogen target will be used to make cross-section measurements of $\gamma_v + p \rightarrow \pi^+ + n$. We will use a liquid deuterium target to determine the separated ratios

$$R_i = \frac{\sigma_i(\gamma_v + n \rightarrow \pi^- + p)}{\sigma_i(\gamma_v + p \rightarrow \pi^+ + n)} \quad i = L, T.$$

The Hall C cryogenic target built by Joe Mitchell's group will be used. The design is similar to that of a SLAC target by John Mark. It is possible to rapidly change between liquid hydrogen, liquid deuterium, or empty vessels. Use of 4 cm cells is essential due to the limited SOS target acceptance. The target windows will be viewed by both spectrometers at all angle settings, so target empty measurements must also be made. During the Δ form factor measurement (E94-014) completed in December 1996, the 4cm LH2 target cells saw weeks of continuous operation at 80 μA and 4 GeV. The fast (nominal 20 KHz) raster was used with an amplitude of 1 mm in both X and Y. Our measurements will take place at 100 μA. Above 80 μA at 4 GeV beam energy we are also required to operate the slow raster for beam dump protection. By 1997 we expect the slow raster to be located downstream of the target. [21] If it is not, we will include the current and phase information in our data stream so we can de-raster the data just as is currently done for the fast raster.

Standard Hall C beamline hardware will be used. In addition to the raster systems, superharps permit accurate measurements of beam size and angle. Passive RF cavities absolutely normalized with an Unser monitor and an accurate current reference provide average current measurements with errors of 100-200 nA (ie, 1-2% at 10 μA). Chen Yan's arc energy measurement system will be used to determine the absolute beam energy to .1%. Accelerator BPM information is also available in our data stream via EPICS so we can monitor beam energy drifts (often as much as $5{\cdot}10^{-4}$ due to RF phase instabilities).

2.1 Kinematic Settings

Kinematic settings for $\pi^{\pm}$ detection are found in Table 2 for the approved and proposed measurements. The invariant mass W is constrained to be 1.95 GeV/c^2. These settings were arrived at after a careful study of the accelerator beam energy and Hall C constraints. A minimum number of non-standard beam energies are requested. We assume that 800 MeV/pass and 1 GeV/pass accelerator tunes will both be standard by Fall 1997.

Table 2: Kinematic settings for $N(e,e'\pi^{\pm})N$ and $p(e,e'p)\pi^0$ at Q^2=.5-3.2 and W = 1.95

Q^2 $(GeV/c)^2$	P_e (GeV/c)	ϵ	$\theta_{e'}^{SOS}$ (deg)	θ_h^{HMS} (deg)	$P_{e'}^{SOS}$ (GeV/c)	P_π^{HMS} (GeV/c)	P_p^{HMS} (GeV/c)	$-t_{min}$ $(GeV/c)^2$
APPROVED (E93-021)								
.50	2.445	.42	33.34	10.06	0.621	1.806	.149	.022
	3.545	.76	16.46	14.44	1.721			
.75	2.645	.42	37.44	11.28	0.688	2.140	.212	.044
	3.545	.70	21.03	15.45	1.588			
1.0	2.645	.31	48.75	10.37	0.555	2.317	.270	.071
	3.545	.65	25.44	15.65	1.455			
1.6	3.045	.29	54.10	10.90	0.635	2.722	.396	.151
	4.045	.63	28.47	16.65	1.635			
PROPOSED								
2.4	3.545	.27	58.50	10.78	0.709	3.232	.547	.277
	4.545	.58	32.27	16.40	1.709			
3.2	4.045	.25	60.36	10.53	0.783	3.721	.685	.419
	5.045	.54	34.70	15.83	1.783			

We also wish to look for protons corresponding to forward π^0 production to search for pQCD related longitudinal backgrounds. These backgrounds might also be thought of as arising from minimally inelastic jets. There are two solutions to the proton momentum in $p(e,e'p)\pi^0$ at $\theta_{pq} = 0$ degrees. The lower proton momentum solution corresponds to t-channel absorption of the virtual photon by a virtual pion. When the recoil momenta reach a few hundred MeV/c the resulting protons are detectable in the HMS.

2.2 Rates

Our rate estimates are based on the following constraints:

- The target thickness 4 cm.
- The beam current is 100 μA.
- The total trigger rate (reals + randoms + prescaled singles) assuming a 40 nsec coincidence window should not exceed 1 kHz. Above this rate the data acquisition deadtime will increase dramatically. (We are actually far below this trigger rate in this proposal.)

Table 3: Hall C detection efficiencies.

HMS tracking	.95
SOS tracking	.95
pion absorption	.95
pion decay (typical)	.85
HMS acceptance for δ = -10% to +10%	.9
SOS acceptance for δ = -15% to +15%	.9
TOTAL	.59

The coincidence rate assuming 100 μA on a 4 cm LH2 target (Luminosity = $1 \cdot 10^{38} cm^{-2} sec^{-1}$) is then:

$$R = (1.06 \cdot 10^8)\Gamma_v \frac{d^3\sigma}{d\Omega_e d\Omega_\pi^{cm} dE_e} \frac{d\Omega_\pi^{cm}}{d\Omega_\pi^{lab}} \Delta\Omega_e \Delta\Omega_\pi \Delta P_{e'}$$

where $1.06 \cdot 10^8 = (1 \cdot 10^{38} cm^{-2} sec^{-1})(1 \cdot 10^{-30} cm^2/\mu barn)$. Spectrometer acceptances were already given in Table 1; kinematic settings are found in Table 2; detection efficiencies are found in Table 3; count rate estimates are summarized in Table 4. Note that the above rate formula will generally overpredict the rates found in Table 4 due to the strong peaking of σ_L near $-t_{min}$.

Singles rates in the HMS and SOS were examined for $p(e, e'\pi^+)$ data taking. [22] The total singles rates are well below the capability of the detector packages, which were constructed with multi-MHz singles rates in mind. For the purpose of calculating online random coincidence rates, the HMS trigger rate was taken as equal to the raw trigger rate. (We do not distinguish pions and protons in the HMS online.) The SOS trigger rate was that for electrons only. The random coincidence rate is then given by (HMS trigger rate)(SOS trigger rate)Δt, where the coincidence resolving time Δt = 40 nsec. The resulting online real + random rates are well below the capability of our data acquisition system. Offline, the relevant resolving time is 2 nsec and the reals to randoms ratio for electron-pion coincidences after missing mass cuts will only be a few percent for $p(e, e'\pi^+)$. Random backgrounds will be an order of magnitude larger for $d(e, e'\pi^\pm)$ because of the larger missing mass cut necessary.

2.3 Particle Identification

The HMS will sit at very forward angles throughout the experiment. The detector package will be configured for $\pi^\pm$ or proton detection in this experiment, the two polarities presenting very different cases for particle identification. In the positive polarity case, the ratio π/p is of order 1. Positron rates are negligible. When the HMS is tuned for π^-, the ratio e/π varies from 1 to 10.

Table 4: Real coincidence rate in parallel kinematics for the $N(e, e'\pi^{\pm})N$ kinematic settings based on a MCEEP simulation with the actual acceptances. A 4cm LH2 target and 100 μA are assumed. The detection efficiency assumed is .59 .

Q^2	P_e (GeV/c)	σ (pb/sr^2 $/MeV$)	Γ_v (/GeV)	$d\Omega^{cm}$ $/d\Omega^{lab}$	Rate (Hz)	$\Delta Q^2 \Delta W$ Cut Effi.	Hours per 10,000 /Det.Effic. /Cut Effic.
APPROVED (E93-021)							
.50	2.445	14.43	.507e-3	5.08	12.68	1.0	0.37
	3.545	103.4	.231e-2		171.2	.26	0.11
.75	2.645	9.134	.343e-3	5.79	8.889	1.0	0.53
	3.545	45.46	.116e-2		80.11	.30	0.20
1.0	2.645	3.549	.176e-3	6.54	2.786	1.0	1.69
	3.545	21.07	.669e-3		37.46	.24	0.52
1.6	3.045	1.670	.106e-3	8.43	1.500	1.0	3.14
	4.045	8.526	.390e-3		16.28	.27	1.07
PROPOSED							
2.4	3.545	0.594	.656e-4	11.24	0.595	1.0	7.91
	4.545	2.724	.213e-3		5.330	.30	2.94
3.2	4.045	0.409	.468e-4	14.35	0.440	1.0	10.70
	5.045	1.550	.139e-3		3.023	.35	4.45

The detector consists of two wire chambers followed by an X-Y scintillator hodoscope, a gas Cerenkov detector, another X-Y hodoscope, and finally a Pb-glass shower counter. Using C_4F_{10} in the gas Cerenkov we are able to tune the velocity threshold throughout our momentum range by changing the vessel pressure. When operated at about .5 atmospheres, only electrons will emit light in this experiment, so the Cerenkov will be used in the hardware trigger to reject electrons for $(e, e'\pi^-)$ measurements at low Q^2. Offline the Pb glass shower counter will be used to further reduce electron contamination. In combination the gas Cerenkov and the Pb glass shower counter will allow us to reject electrons with efficiencies orders of magnitude better than is needed. The primary (non-prescaled) HMS trigger for π^+ or p detection will be simply $S1 \bullet S2$. Only 3 of 4 scintillator arrays require hits so the efficiency is 100% even with a dead phototube. For π^- detection the trigger may be tightened to $S1 \bullet S2 \bullet (NoElectron)$.

The SOS detector package will be configured for electron detection. Both the Yerevan shower counter and the U. Colorado Cerenkov filled with freon at 1 atmosphere will be used. Because the SOS angle will vary from forward to backward angles, the ratio π^-/e varies varies from one to several hundred. We plan to reject pions at the hardware level, allowing only prescaled sample of pions to pass to monitor the trigger efficiency. The Hall C electron trigger is a conservative one copied after the NE18 experiment which identifies an electron as either a high preshower signal or a high gas Cerenkov signal. In this case the primary (non-prescaled) SOS trigger will be $S1 \bullet S2 \bullet Electron$.

While the event of interest will be HMS•SOS, prescaled HMS and SOS singles events will also be taken in order to monitor the detector and trigger efficiencies and luminosity.

Offline particle identification is done as follows: First, most protons in the HMS are removed by a time of flight mass measurement defined as

$$(TOF\ Mass)^2 = P^2(\frac{1}{\beta^2} - 1)$$

Mass discrimination is excellent since the meantime resolution per array is roughly 100 psec (or $\sigma_\beta = .017$). A plot showing the mass separation in the HMS for $Q^2 = 1.6$ from the October 1996 test run is found in Figure 4. Failure to make this cut would allow random protons to underlie the real $(e, e'\pi)$ peak in the final coincidence time spectrum. The small percentage of real coincident protons which pass the $(TOFMass)^2$ cut at $Q^2 = 2.4$ and 3.2 are roughly 3 nsec away from the real pion peak. (Table 5) This is a huge separation when compared to our coincidence timing resolution of better than 166 psec (σ), so these protons are easily removed. A plot showing the coincidence timing resolution is found in Figure 5. The beam current of the test run was only 1/4 that of the proposed experiment,

2.4 Non-physics backgrounds

Once a combination of on-line hardware and off-line software have determined that there was a coincidence between an electron in the SOS and a hadron in the HMS (a pion or proton depending

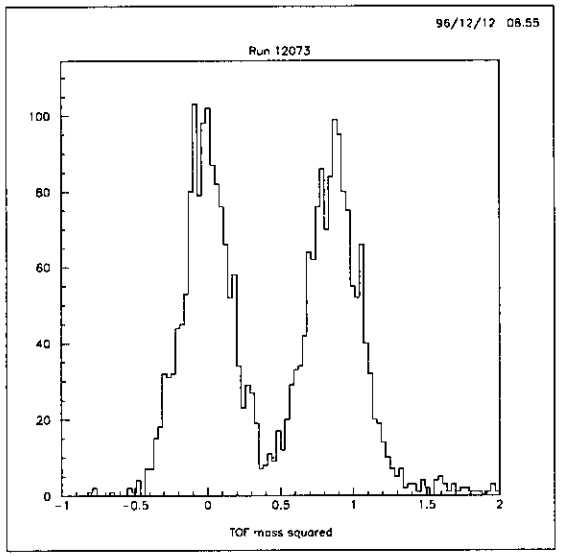

Figure 4: Square of the HMS TOF mass. Pions and protons are well-separated at 2.722 GeV/c.

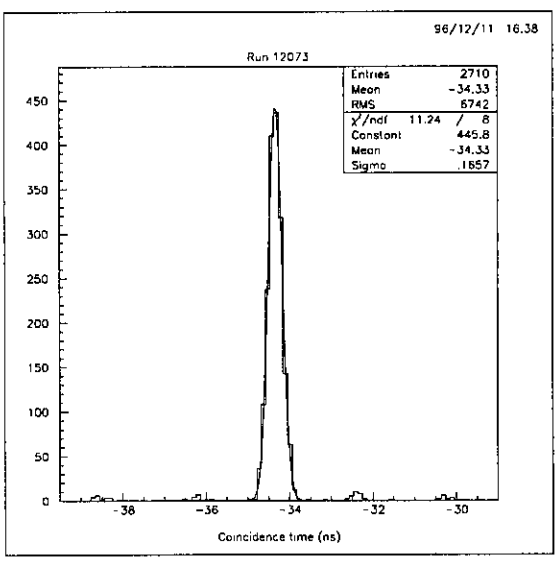

Figure 5: HMS-SOS coincidence time resolution for $p(e, e'\pi^+)n$. The offline missing mass cut was made wider than necessary so that random coincidences would be visible.

Table 5: Velocity, TOF, and pion survival fraction for each kinematic setting.

Q^2	P_π (GeV/c)	β_π	Pion Survival Fraction (27m)	β_p	TOF_p (nsec)	$TOF_p - TOF_\pi$ (ns)
APPROVED (E93-021)						
.50	1.806	.9970	.7653	.8874	101.42	11.3
.75	2.140	.9979	.7979	.9158	98.27	8.2
1.0	2.317	.9982	.8118	.9269	97.10	7.0
1.6	2.722	.9987	.8374	.9454	95.20	5.1
PROPOSED						
2.4	3.232	.9991	.8612	.9603	93.72	3.6
3.2	3.721	.9993	.8782	.9696	92.82	2.7

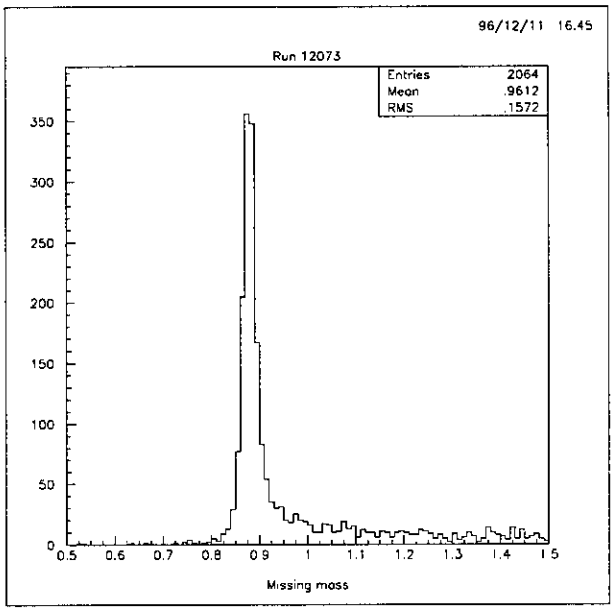

Figure 6: Reconstructed neutron mass from $p(e, e'\pi^+)n$. The optics reconstruction matrix elements are not optimized which causes the neutron mass to be offset.

on the reaction), there remain several backgrounds of the incoherent 'non-physics' variety: random coincidences and events from the target endcaps.

The online coincidence resolving window will be roughly 40 nsec. Because the offline analysis will allow the beam burst to be determined, the relevant resolving time becomes 2 nsec. Some of the remaining randoms may be removed with vertex cuts, but most randoms will be removed with missing mass cuts. The mass of the residual (ie, undetected) hadron may be reconstructed from the final electron and detected hadron 4-momenta:

$$M_{res}^2 = P_{res}^2 = (P_e - P_{e'} + P_{tgt} - P_h)^2$$

A cut on this missing mass variable would remove backgrounds with larger inelasticity, such as radiative tails and two pion production. (Figure 6)

We have chosen the target length to be relatively short. This means that both spectrometers will view the endwindows in all configurations, so background runs and subtractions will be necessary. Since the aluminum windows are each 4 mils thick, the ratio of protons in the windows to protons in the liquid hydrogen is about 10%. Assuming a factor of 2 reduction for final state interactions, the expected background is roughly 5%. The measured background in the October 1996 test run was about 3% for a wide open missing mass cut appropriate to $d(e, e'\pi^\pm)$ but less than 1% for a tight missing mass cut appropriate for $p(e, e'\pi^+)$. Since the Hall C "empty" target consists of two

Table 6: Beam request for hydrogen and deuterium running. The number of hours per setting is the parallel kinematic estimate doubled to allow for measurements at higher $-t$.

Q^2	LH2 Hours $p(e,e'\pi^+)$	LH2 Hours $p(e,e'p)\pi^0$	LD2 Hours $d(e,e'\pi^+)$	LD2 Hours $d(e,e'\pi^-)$	Overhead Hours	Total Hours
PROPOSED						
2.4	15.8	15.8	15.8	15.8	24	87.2
	5.9	5.9	5.9	5.9	24	47.6
3.2	21.4	21.4	21.4	21.4	24	109.6
	8.9	8.9	8.9	8.9	24	59.6
Total						304 (12.7 days)

40 mil thick Aluminium windows separated by 4 cm, which can tolerate up to 50 μA, the "empty" data come in 5 times = (40 mil $\times$ 50 μA)/(4 mil $\times$ 100 μA) faster than window events on the real target. Thus, empty target overhead is negligible.

2.5 Beam Request

The beam request assumes $1{\cdot}10^4$ counts per parallel kinematic setting including detection inefficiencies and cut inefficiencies. (Much of the raw rate for the forward electron angle setting is due to Q^2 and W values which cannot be matched to the smaller phase space of the backward angle setting.) An equal time is allocated for measurements at larger $-t$ to aid in the extrapolation to the pole. We take $p(e,e'\pi^+)$ and $p(e,e'p)\pi^0$ running times on LH2 to be equal. We also take the $d(e,e'\pi^+)nn_s$ and $d(e,e'\pi^-)pp_s$ running times to be equal to the $p(e,e'\pi^+)$ time so that accurate values of the separated ratios $\sigma(\pi^-)/\sigma(\pi^+)$ can be obtained. Additional time is requested for allowable overhead (ie, we assume nothing breaks in Hall C or in the accelerator). Our overhead assumes 2 shifts to tune 5.045 GeV, 3 shifts to tune 4.545 GeV, one shift for each of 4 kinematic settings for angle, target, and momentum changes, and 3 shifts for elastic checkout and sieve runs to find new HMS matrix elements. (This was an oversight in the E93-021 proposal.) A summary of the beam request is contained in Table 6. *We request 12.7 additional days of beam time during the Fall 1997 running cycle to make measurements at Q^2 = 2.4 and 3.2 .*

2.6 Errors

Two measurements at fixed (Q^2, W) and different values of ϵ, the virtual photon polarization, are needed in order to determine σ_L. Thus if $\sigma_1 = \sigma_T + \epsilon_1\sigma_L$ and $\sigma_2 = \sigma_T + \epsilon_2\sigma_L$ then

$$\sigma_L = \frac{1}{\epsilon_1 - \epsilon_2}(\sigma_1 - \sigma_2).$$

Assuming uncorrelated errors in the measurement of σ_1 and σ_2, then

$$\frac{\Delta\sigma_L}{\sigma_L} = \frac{1}{(\epsilon_1 - \epsilon_2)}\frac{1}{\sigma_L}\sqrt{\Delta\sigma_1^2 + \Delta\sigma_2^2}.$$

A more insightful expression is obtained by defining $R \equiv \sigma_T/\sigma_L$ and $\Delta\sigma/\sigma \equiv \Delta\sigma_1/\sigma_1 = \Delta\sigma_2/\sigma_2$, then

$$\frac{\Delta\sigma_L}{\sigma_L} = \frac{1}{\epsilon_1 - \epsilon_2}\frac{\Delta\sigma}{\sigma}\sqrt{(R+\epsilon_1)^2 + (R+\epsilon_2)^2}$$

This equation makes explicit the error amplification due to a limited ϵ range as well as a large R. For the proposed experiment, $R \leq 1$, so a limited ϵ lever arm is the primary source of error amplification. Systematic errors in the kinematic factors (ie, Γ, Q^2, W^2, and ϵ) are small provided we determine the absolute P_e to $1 \cdot 10^{-3}$ and the centroids of laboratory scattering angles to 1 mrad.

Based on the experience of the SLAC group [19], it will require a great deal of effort at TJNAF to achieve 2% absolute cross section errors with extended targets and magnetic spectrometers with multiple solid angle-defining apertures. The SLAC estimate of 2% systematic errors was obtained by adding the errors in target thickness, acceptance, beam charge, and radiative corrections in quadrature:

$$\sqrt{.01^2(target) + .01^2(acceptance) + .01^2(charge) + .01^2(rad.corr.)} = 2\%.$$

We believe a reasonable goal for the error $\Delta\sigma/\sigma$ for the early years at TJNAF is

$$\sqrt{.02^2(target) + .02^2(acceptance) + .005^2(charge) + .01^2(rad.corr.)} \sim 3\%.$$

Table 7 gives our anticipated errors for the entire Q^2 range, including both systematic and statistical errors. Statistical errrors are negligible for all Q^2.

Assuming the absolute cross section error appropriate for TJNAF, and a value of .1 (.5) for σ_T/σ_L for the low (high) Q^2 settings, then $\Delta\sigma_L/\sigma_L = 8.0\%$ (15%). Since $\sigma_L \propto F_\pi^2$ we have

$$\frac{\Delta F_\pi}{F_\pi} = \frac{1}{2}\frac{\Delta\sigma_L}{\sigma_L} = 4.0\% - 7.5\%.$$

We would like to point out that if errors in the measurement of σ_1 and σ_2 are correlated (eg, the beam current monitor calibration is consistently .5% low) then the error in F_π will be smaller than that given above. However, our error estimates neglect any model uncertainties and physics backgrounds. We will determine these in the experiment and include these in the final published errors on F_π. Given these caveats, our expected uncertainties are shown in Figure 7.

Table 7: Expected errors for F_π in the proposed experiment. Systematic and statistical errors assumed are 3% and 1%, respectively. Model errors are not included.

Q^2	$\Delta\epsilon$	σ_T/σ_L	$\Delta F_\pi/F_\pi$ (%)
APPROVED (E93-021)			
.50	.34	.1	4.8
.75	.28	.1	5.3
1.0	.34	.1	4.1
1.6	.34	.1	4.0
PROPOSED			
2.4	.31	.5	6.8
3.2	.29	.5	7.2

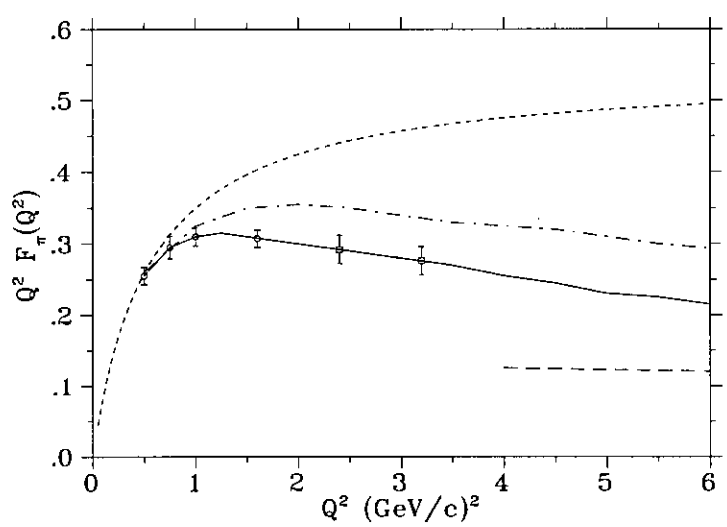

Figure 7: Our *anticipated* errors for F_π assuming the Bethe-Salpeter equation model of Jacob and Kisslinger (solid line). The other theory curves are the same as in Figure 1.

2.7 The Collaboration

We believe our collaboration has the strength, commitment, and experience to successfully carry out these measurements. The collaboration has grown in size since the original proposal. There are now three cospokespersons and three thesis students on this experiment. This reflects not only a growing interest in the measurement of F_π, but the reality of carrying out a large experiment and subsequent data analysis. Hampton University recently completed data taking on kaon electroproduction in Hall C, and RPI recently completed data taking on the Δ form factor at $Q^2 = 4$.

This collaboration appropriately brings together many of the people who built Hall C: Hampton University built the HMS wire chambers, Old Dominion University built the SOS scintillator hodoscopes, RPI contributed heavily to the SOS Wire Chamber installation and commissioning, and Yerevan built the shower counters in both the HMS and SOS. TJNAF staff scientists assisted in these projects, built the HMS hodoscopes, and were responsible for fast electronics, slow controls, data acquisition, thin window fabrication, spectrometer optics, and beamline hardware.

3 Summary

At TJNAF we have the potential to dramatically improve the F_π database. Much can be learned from the proposed experiment about the usefulness of QCD sum rules and relativistic potential models for understanding the structure of the pion in the (presumably) difficult and non-perturbative Q^2 regime of 1-5 $(GeV/c)^2$.

All the hardware required for the proposed experiment is in place. The HMS quad string must be pulled back 40 cm to enable operation at angles as small as 10.5 degrees. Rates, backgrounds, and particle identification have been checked in a short test run on $p(e, e'\pi^+)n$ at $Q^2 = 1.6$ at 4.045 GeV beam energy. By Hall C standards, this is a relatively easy experiment. The real rate is relatively large, non-physics backgrounds are small, and particle identification is straightforward. Because 5 GeV beam will be available in Fall 1997, we would like to extend our measurements to $Q^2 = 2.4$ and 3.2 contiguous with our low Q^2 measurements.

Last year we proposed (LOI-95-001) to extend our measurements of F_π to $Q^2 = 5$ in Hall A after the Hall C measurements are complete. Those measurements will require 6 GeV beam energy (minimum) and a thorough understanding of the HRS2 spectrometers and beamline hardware, both of which are still some time from being achieved. We think that the proposed measurements in Hall C at $Q^2 = 2.4$ and 3.2 will allow TJNAF to do the best physics at this point in the life of the laboratory. It is still our intention to extend our measurements to $Q^2 = 5$ in Hall A when the hall and the accelerator are ready.

References

[1] S.R.Amendolia et al., PL **146B**, 116 (1984); NPB**277**, 168 (1986). G.T. Adylov et al., PL **51B**, 402 (1974); NPB**128**, 461 (1977). E.B. Dally et al., PRL **39**, 1176 (1977); PRD **24**, 1718 (1981). E.B. Dally et al. PRL **48**, 375 (1982).

[2] P. Brauel et al., Z. Physik C, **3**, 101 (1979)

[3] Brown et al., Phys. Rev. D **8**, 92 (1973)

[4] F.A. Berends, Phys. Rev. D **1**, 2590 (1970)

[5] C.J. Bebek et al., Phys. Rev. D **9**, 1229 (1974)

[6] C.J. Bebek et al., Phys. Rev. D **13**, 25 (1976)

[7] C.J. Bebek et al., Phys. Rev. Lett. **37**, 1326 (1976); and Phys. Rev. D **17**, 1693 (1978)

[8] O. Nachtmann, Nucl. Phys. **B115** 61 (1976).

[9] N. Isgur and C.H. Llewellyn Smith, Phys. Rev. Lett. **52**, 1080 (1984), Phys. Lett. **B217**, 535 (1989), and Nucl. Phys. **B317** 526 (1989).

[10] A.P. Bakulev and A.V. Radyushkin, TJNAF preprint.

[11] S.V. Mikhailov and A.V. Radyushkin, TJNAF preprint.

[12] O.C. Jacob and L.S. Kisslinger, Phys. Lett. B **243**, 323 (1990).

[13] G. R. Farrar and D. R. Jackson, Phys. Rev. Lett. **43**, 246 (1979).

[14] H. Ito et al., Phys. Rev C **45**, 1918 (1992).

[15] C.-R. Ji and F. Amiri, Phys. Rev. D **42** 3764 (1990).

[16] T. Draper, R.M. Woloshyn, W. Wilcox, and K.-F. Liu, Nucl. Phys. **B318**, 319 (1989).

[17] W. Wilcox, private communication.

[18] C.E. Carlson and J. Milana, Phys. Rev. Lett. **65**, 1717 (1990).

[19] P.E. Bosted et al., Phys. Rev. Lett. **68**, 3841 (1992).

[20] "Report on the acceptances, optical properties, and resolution of the lean mode for HMS", J. Volmer and H. Blok, September 30, 1996, private communication.

[21] Chen Yan, private communication.

[22] J. O'Connell and J. Lightbody, Comp. in Phys. May-June **57** (1988)